

Minimum-Time Path Planning for Autonomous Landing of UAV on Aerial Drone Carrier

Morteza Alijani¹ and Anas Osman²

Abstract—The motivation for this work stems from the need to develop trajectory planning algorithms for small UAVs with limited resources. The goal is to address one of the most critical problems in UAV design, namely weight constraints. Therefore, in order to reduce the weight, small batteries are used which affect the flight duration and overall performance. To increase the operating time during a mission, frequent recharging is typically required. To solve this problem, an autonomous air-to-air take-off and landing on a drone carrier for recharging is proposed. The main objective of this study is to calculate the minimum time and thus the shortest maneuver route between the UAV and the drone carrier. To achieve this goal, the path planning algorithm is utilized through the closed-loop direct optimal control approach to calculate the optimal time, which is defined as a cost function. In addition to the optimization techniques, the singular perturbation technique (SPT) and the Hamiltonian are used to solve and refine the optimal control problem (OCP). Finally, the numerical simulation results in both open and closed loop are presented and the performance of the proposed algorithm is evaluated.

Index Terms—Autonomous air-to-air landing, Aerial drone carrier, Optimal control problem (OCP), Unmanned aerial vehicle (UAV), Path planning

I. INTRODUCTION

Recently, technology has made an impressive leap in development and innovation, which has led to a noticeable demand for new technologies, especially Unmanned Aerial Vehicles (UAVs). The UAV is an aircraft that can be flown autonomously or remotely from the ground without a pilot on board. Over the past few years, UAVs have gained increasing popularity in both civil and military operations. UAVs are thriving in practical applications such as wildlife monitoring [1], disease control [2], search and rescue [3], delivery services at Amazon and Google in the US [4,5], DHL-Postdienst in Germany [6], Smart Dust [7] and military services [8]. Nevertheless, the implementation of the system with UAVs is limited by battery power in terms of capacity and flight time. During search and rescue missions, for example, these small UAVs are exposed to considerable risk due to battery constraints, resulting in frequent downtimes for recharging. One of the latest techniques proposed by researchers to tackle this issue is autonomous take-off and landing on a mobile platform that can be used for recharging [9]. In this scenario, the operation is performed automatically without human intervention. The primary goal of this approach is to ensure continuous operation and an extension of the flight

time of the UAV without any disturbances. This technique has already been applied in many cases, such as autonomous take-off and landing on a moving aircraft carrier [10] and vessels [11]. Moreover, studies have recently been carried out that include the implementation of a free autonomous landing system Global Navigation Satellite System (GNSS), which allows the UAVs to land safely on a mobile platform [12], [13]. Vision-based autonomous landing techniques also suggest a target tracking system that can land on a moving platform [9]. The same is true for air-to-air refueling, which has achieved an extraordinary degree of research popularity, especially through the continuous connection of Air-to-Air Autonomous Refueling (AAAR) with the military sector. Air-to-air refueling has proven to be effective in extending flight range and endurance [13].

On the other hand, one of the main challenges for intelligent UAV development is path planning [14]. Taking into account the battery limitations on the UAV, it is necessary to identify the shortest route for manoeuvres of UAVs, since the power consumed during manoeuvres is closely linked to the length of the flight path. The motivation behind path planning methods in UAVs is not only to find an optimal solution but also to provide UAVs with a collision-free orbit. Typically, the process of extracting the optimal path and the corresponding optimal control signal is divided into two main categories, namely open-loop and closed-loop optimization, since many different algorithms have been developed for each technique. Closed-loop optimization itself can be divided into linear and nonlinear optimization, depending on the nature of the dynamics of the system subject to the optimization process. For example, in [15], the authors use the nonlinear model predictive control approach based on a geometric representation of the error to track the posture of the multirotor Micro Aerial Vehicle (MAV) based on the SO(3) special orthogonal group. Recently, some closed-loop nonlinear optimization algorithms have also been developed, which introduce full feedback nonlinear model prediction control that combines trajectory optimization and tracking control into a single unified approach. The Sequential Linear Quadratic used in a Model Predictive Control (SLQ-MPC) to solve a nonlinear optimal control problem and perform an experiment with the full system dynamics of the MAV [16]. Although the closed-loop system can be robustly controlled against external disturbances, the optimization is dynamically unacceptable because the optimization process can only be applied to the error part of the UAV dynamics, while in the case of open-loop optimization, more effective optimization can be realized since the optimization is performed for the main dynamics of the system [16,17].

¹ Morteza Alijani and Anas Osman are students with the Department of Industrial Engineering, University of Trento, Italy. name.surname@studenti.unitn.it

Moreover, the identification of the optimal path of a system can be explained as an optimal control problem for which two main algorithms can be used, including direct and indirect methods. In the direct approach, the parameters involved in the dynamics of the UAV are optimized to obtain an optimal cost function. In indirect methods, on the other hand, the optimization algorithm has to compute variations, which leads to a two-boundary value problem. The indirect method is usually associated with nonlinear systems with complex dynamics, since they can benefit from the analytical capabilities of the indirect approach. The direct method, however, is a numerical method that considers only linear systems that can be directly optimized [17].

The main contribution of this paper is to propose a direct closed-loop optimization method, which is a numerical method for determining the optimal path and the associated optimal control of the UAV. The proposed optimization method is a Hamiltonian method based on a numerical approach. The reason for choosing this technique is that there is no specific algorithm that can define an optimal path for the UAVs. Therefore, due to the linear model and experimental setup, we choose numerical methods since an exact model of the system is not available and path planning can be performed offline in our proposed algorithm [17].

The rest of this paper is organised as follows. We have presented the dynamic model of the UAV in Section II. The optimal control solution using Hamilton's principle and singular perturbation technique is described in detail in Section III. The numerical simulation, results and conclusion are discussed in Section IV and Section V, respectively.

II. DYNAMICAL MODEL

In this section we demonstrate the dynamic system of the UAV with forces in detail. We use the simplified model of the UAV to obtain a feasible closed-loop solution. The formulation of the problem is done through the construction of the dynamic model illustrated in Figure 1. In this study, the spatial coordinate system of the UAV and aerial platform has been established in the (2D) X-Y axis demonstrated in Figure 2. The X-axis and the Y-axis are in the same vertical plane, X-axis is perpendicular to the Y-axis. The UAV and aerial (Drone) carrier have the same direction and positive in X-axis. The equations describing the motion of the UAV in the vertical plane are presented in (1) to (7) [18]. By considering the Figure 1, in these formulas, point u represents the position of the UAV and point d depicts the position of the Drone carrier, while vector v_u and v_d illustrates the velocity of UAV and drone carrier, respectively. (x_u, y_u) and (x_d, y_d) are respectively the positions of the UAV and Carrier, M_u is the total mass of the UAV, θ_u represents the interceptor's heading angle (the UAV), T_F is the total thrust force of the UAV produced by 4-rotors, D_F , and F_L are the total drag force and total lift force that affect the UAV, accordingly. Finally, α is the angle of attack of the UAV which is variable and related to the landing direction. Additionally, in formula 6, ρ is the air density, s is the reference area of the UAV and cl is

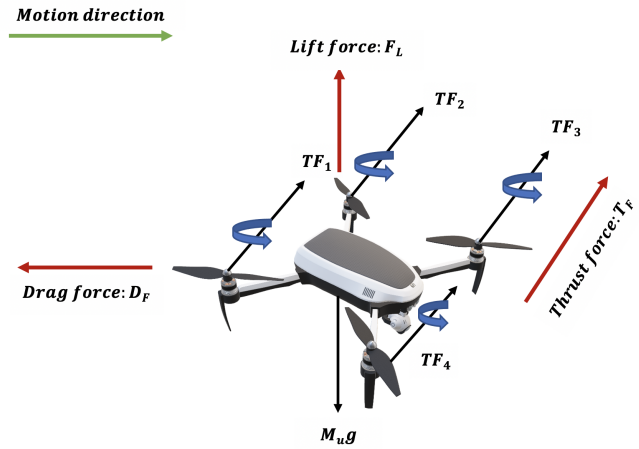


Fig. 1. The free body diagram of the UAV with forces

the lift coefficient related to the angle of attack. Further, from a control point of view, in order to successfully control the UAV, the normal acceleration required during landing should be equal to the normal acceleration which the UAV actually generates during the landing process. Therefore, for satisfying this condition, the acceleration is presented in formula (7) [18].

$$\frac{dx_u}{dt} = v_u \cos \theta_u \quad (1)$$

$$\frac{dy_u}{dt} = v_u \sin \theta_u \quad (2)$$

$$\frac{d\theta_u}{dt} = \frac{T_F \sin \alpha + F_L}{M_u v_u} - \frac{g \cos \theta_u}{v_u} \quad (3)$$

$$\frac{dv_u}{dt} = \frac{T_F \cos \alpha - D_F}{M_u} - g \sin \theta_u \quad (4)$$

$$a_n = \frac{T_F \sin \alpha + F_L}{M_u} - g \cos \theta_u \quad (5)$$

$$F_L = \frac{1}{2} \rho s c_l v_u^2 \quad (6)$$

$$a_r = \frac{T_F \sin \alpha + F_L}{M_u} - g \cos \theta_u \quad (7)$$

III. PROBLEM FORMULATION

This section contains the mathematical formulation of the optimal control problem (OCP) to achieve the goal considered in this paper. We assume that the path planning environment for the UAV is free of static and dynamic obstacles, which is the primary assumption in this study to reduce the complexity of the computation. Formulas presented in the following section are based on Figure 2 and Figure 3. To calculate the minimum time, we suppose that the UAV (interceptor) is flying

at a constant speed of v_u in the horizontal plane. Its objective is to reach the target (Drone Carrier), flying at a constant velocity of v_d in a given direction. For describing the motion, we used a coordinate system with an origin at the interceptor's center-of-mass and with X-Axis direction parallel to the target's constant velocity vector (Figure 2). The equations of motion illustrated at Figure 2 including the UAV and the drone carrier are as follows:

$$\frac{dx}{dt} = v_d - v_u \cos \theta_u \quad (8)$$

$$\frac{dy}{dt} = -v_u \sin \theta_u \quad (9)$$

$$\frac{d\theta_u}{dt} = \tilde{\lambda} c \quad (10)$$

$$\tilde{\lambda} = \frac{v_u}{R_c} \quad (11)$$

where x and y are relative displacements, θ_u is the interceptor's heading angle, and R_c is the minimum turning radius of the interceptor. The variable c is the controller and its magnitude is bounded by unity, $|c| \leq 1$. For simplifying the problem, the time dependency of all variables has been eliminated. We initiate the process at $t_0 = 0$ to t_f in the following optimal control problem (OCP).

minimize:

$$\varphi(x(t_0), x(t_f)) + \int_{t_0}^{t_f} f_0(t, x(t), c(t)) dt$$

subject to equations (8-11) and the following boundary conditions:

$$\begin{aligned} x(0) &= 0 \\ x(t_f) &= 0 \\ y(0) &= y_0 \\ y(t_f) &= 0 \\ \theta_u(0) &= 0 \\ \theta_u(t_f) &= free \end{aligned} \quad (12)$$

The primary purpose of the cost function in this paper is dedicated to finding the minimum time required for the UAV to reach the charging platform while imposing a soft bound on the control variable via a positive weighting factor β and quadratic form. This factor can be used to ensure that the control remains within its prescribed bounds. Consequently, the objective function in optimal control problem (Bloza problem) is presented as follows:

minimize:

$$D = t_f + \int_0^{t_f} (\beta c^2) dt \quad (13)$$

subject to equations (8-11) and set of boundary conditions on (12). In order to scale the problem, we used the unit distance of R_0 in formula (14) as the initial separation range between the UAV (interceptor) and drone carrier (target) as follows:

$$R_0 = \sqrt{x_0^2 + y_0^2} \quad (14)$$

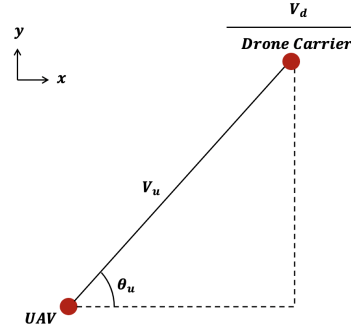


Fig. 2. The schematic diagram of the UAV and the Drone Carrier in X-Y axis

By considering this separation unit, the right-hand side of the first two equations (8) and (9) will be of the order of $\frac{v_u}{R_c}$ and $\frac{v_d}{R_c}$. Furthermore, we assumed that $R_0 \gg R_c$, (as in the case in many interception scenarios), and then we can define a small parameters like δ as the ratio between the two parameters R_0 and R_c . Taking to account that the more maneuverable the interceptor is, the smaller δ becomes. Then, by multiplying the equation (10) by δ its right-hand sides becomes of the order of $\frac{v_u}{R_c}$ as do the first two equations (8) and (9). Finally, we introduced a new variable Υ in order to transfer the OCP in (13) to the Mayer's formulation as follows:

minimize:

$$D = t_f + \Upsilon(t_f)$$

subject to:

$$\begin{aligned} \frac{d\Upsilon}{dt} &= \Upsilon'(t) = \beta c^2 \\ \frac{dx}{dt} &= x'(t) = v_d - v_u \cos \theta_u \\ \frac{dy}{dt} &= y'(t) = -v_u \sin \theta_u \\ \delta \frac{d\theta_u}{dt} &= \lambda c \\ \Upsilon(0) &= 0 \\ \lambda &= \frac{R_c}{R_0} \tilde{\lambda} \end{aligned} \quad (15)$$

The solution to the OCP problem presented in (15), various approaches may be used. In this study, we employed the Hamiltonian principle technique. The Hamiltonian is a function used to solve the optimal control problem of a dynamic system. It can be observed as an instantaneous increment of the Lagrangian expression of a problem that can be optimized over a certain time horizon. By using the definition of principle the Hamiltonian function H and B for boundary value problem (BVP) [19], we have:

$$\begin{aligned} H(t, x, c, \theta_u, \mu_x, \mu_y, \mu_{\theta_u}) &= f_0(t, x, c) + \mu_x(x'(t)) \\ &+ \mu_y(y'(t)) + \mu_{\theta_u}(\delta \theta'_u) \end{aligned} \quad (16)$$

By putting the related equation from (15) in (16), the Hamiltonian function computed as follows:

$$H(t, x, c, \theta_u, \mu_x, \mu_y, \mu_{\theta_u}) = \mu_{\gamma}(\beta c^2) + \mu_x(v_d - v_u \cos \theta_u) + \mu_y(-v_u \sin \theta_u) + \mu_{\theta_u} \lambda c \quad (17)$$

Now because:

$$\mu'_{\gamma} = -\frac{\partial H}{\partial \gamma} = 0 \quad (18)$$

and from the transversality condition we have:

$$D\gamma_f = \mu_0 \quad (19)$$

Then, we can obtain that:

$$D\gamma = \mu_0 \quad (20)$$

By taking to account the autonomous conditions in our problem we can have:

$$D_{t_f} = \mu_0 = -H(t_f) = -H(t) \quad (21)$$

Thus, the Hamiltonian is equal to μ_0 , and the remaining ad-joint equations are as follows:

$$\mu'_x = -\frac{\partial H}{\partial x} = 0 \quad (22)$$

$$\mu'_y = -\frac{\partial H}{\partial y} = 0 \quad (23)$$

$$\delta \mu'_{\theta_u} = -\frac{\partial H}{\partial \theta_u} = 0 \quad (24)$$

From (24), we have:

$$-\mu_x v_u \sin \theta_u + \mu_y v_u \cos \theta_u = 0 \quad (25)$$

Finally, the control equation is:

$$\frac{\partial H}{\partial c} = 2\beta \mu_0 c + \mu_{\theta_u} \lambda = 0 \Rightarrow c(t) = \frac{-\mu_{\theta_u} \lambda}{2\beta \mu_0} \quad (26)$$

The next step is dedicated to finding the $\dot{\theta}_u$ corresponding to the triangular collision in Figure 3 between the UAV and the drone carrier, which first illustrates the path from the point of view of an astatic observer located at the initial position of the UAV, then defines the collision triangle between the two moving objects from an initial to a final configuration and determines where they would interact with each other. Based on the collision triangle and taking into account that the line of sight should not rotate with respect to the law of parallel navigation [20], we approached $\dot{\theta}_u$ as follows:

$$v_u \sin(\gamma) - v_d \sin(\Phi) = 0 \Rightarrow \sin(\Phi) = \frac{y_0}{\sqrt{x_0^2 + y_0^2}}$$

$$\Rightarrow v_u \sin(\gamma) - v_d \frac{y_0}{\sqrt{x_0^2 + y_0^2}} = 0$$

$$\Rightarrow \sin(\gamma) = \frac{y_0}{\sqrt{x_0^2 + y_0^2}} \left(\frac{v_d}{v_u} \right)$$

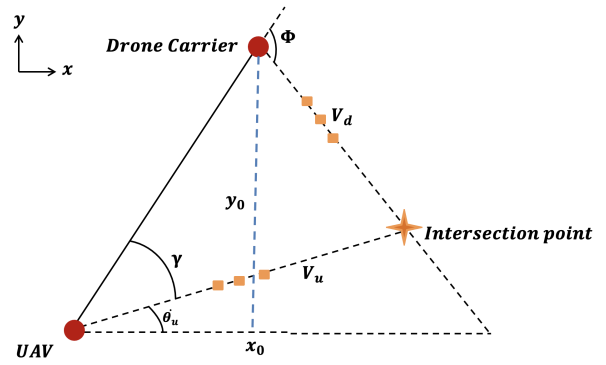


Fig. 3. Collision triangle

$$\dot{\theta}_u = \Phi - \gamma = \arctan\left(\frac{y_0}{x_0}\right) - \arcsin\left[\frac{y_0}{\sqrt{x_0^2 + y_0^2}} \left(\frac{v_d}{v_u}\right)\right] \quad (27)$$

Finally, based on equation (26, 27), we derived μ_0 from the ad-joint variables required for the Hamiltonian function by using $E > 0$, to compute the μ'_x and μ'_y as follows:

$$\begin{aligned} \mu'_x &= E \cos \dot{\theta}_u \\ \mu'_y &= E \sin \dot{\theta}_u \\ E &= \frac{\mu_0}{v_u - v_d \cos \dot{\theta}_u} \end{aligned} \quad (28)$$

For the calculation of the t_f on the basis of the collision triangle, we have chosen a technique of order reduction in connection with the singular perturbation technique (SPT), which is particularly noticeable in the design of the optimal control, which requires the solution of state and cost functions including initial and final conditions [21]. Consequently, by applying the method of order reduction in equations (8-10) we have found:

$$\frac{d\dot{x}}{dt} = v_d - v_u \cos \dot{\theta}_u \quad (29)$$

$$\frac{d\dot{y}}{dt} = -v_u \sin \dot{\theta}_u \quad (30)$$

$$0 = \lambda \dot{c} \quad (31)$$

$$\frac{d\mu_x}{dt} = 0 \quad (32)$$

$$\frac{d\mu_y}{dt} = 0 \quad (33)$$

$$0 = -\mu_x v_u \sin \dot{\theta}_u + \mu_y v_u \sin \dot{\theta}_u \quad (34)$$

Taking to account that, $\dot{u} = 0$, $\dot{\mu}_u = 0$, and $\dot{\theta}_u$ is constant. In order to intercept the target (Drone carrier) at t_f , the following conditions are required:

$$x_f = x_0 + (v_d - v_u \cos \dot{\theta}_u) t_f \quad (35)$$

$$y_f = y_0 + (-v_u \sin \dot{\theta}_u) t_f \quad (36)$$

Finally, from (36), we have:

$$t_f = \frac{x_0}{v_u \cos \dot{\theta}_u - v_d} \quad (37)$$

TABLE I
NUMERICAL PARAMETERS FOR THE SMALL UAV AND DRONE CARRIER

Symbol	Values	Parameter's name
x_0	28.666 ft	Initial Position
y_0	32.569 ft	Initial Position
v_u	45 ft/s	Small Drone's Average Velocity
v_d	80 ft/s	Drone Carrier's Average Velocity
β	3.5	Weighting factor
λ	0.02	Multiplier

We use practical data based on an average Dji Mavic Pro drone [22].

IV. NUMERICAL AND SIMULATION RESULTS

To evaluate the performance of our solution and determine the minimum time a UAV needs to intersect the Drone Carrier. From the experimental parameters proposed in Table 1, we considered two case studies with open and closed loop control at $\delta = 0.08$, which were selected for a moderately maneuverable UAV (Interceptor). The term "closed-loop" or "feedback form" means that instead of making one attempt to solve the problem at t_0 with the given fixed x_0 and y_0 with a fixed $\dot{\theta}_u$, we repeatedly update the value of $\dot{\theta}_u$ with the current measures of x_0 and y_0 . Ultimately, this should greatly improve the accuracy of the results. In addition, β (multiplier) has been adjusted so that the hard limit of control is not violated. Figure 4, presents the path of the initial state in both open and closed loop. (it is illustrated in the reference system of the interceptor). Figures 5 and 6 show the time records of the heading and control. As demonstrated, both controls resemble a similar approach, however, in terms of path planning both open and closed loop tend to significantly differ, especially in satisfying the end conditions of the interception. In order to correct these, higher-order terms are implemented, for the control to remain in open loop. In the second case, however, the results look very similar and the control system is practically indistinguishable from the controller. This is not surprising, because we know that we are approaching the Zermelo's problem when the UAV is highly manoeuvrable, so we use the Singular perturbation technique (SPT) to reduce this problem. The interception problem is solved to the first order for both open-loop and feedback-loop. The open-loop solution applies to systems with initial and/or final boundary layer, whereas the closed-loop solution can be applied to problems with initial boundary layer only. One of the major advantages of the SPT is the on-board implementation of optimal control techniques as direct inputs to the autonomous flight control system. As a result, such an implementation requires the optimal control solution to be obtained in a feedback form. In addition, from Figures (7,4) and Figures (8,5) we can observe that changing the value of δ has an impact on the performance of open-loop and closed-loop, as we decrease the value δ the results are almost identical.

V. CONCLUSION

In this paper, we propose a path planning algorithm for Unmanned Aerial Vehicles (UAVs) to reach the drone carrier for recharging through air-to-air landing. We calculate the

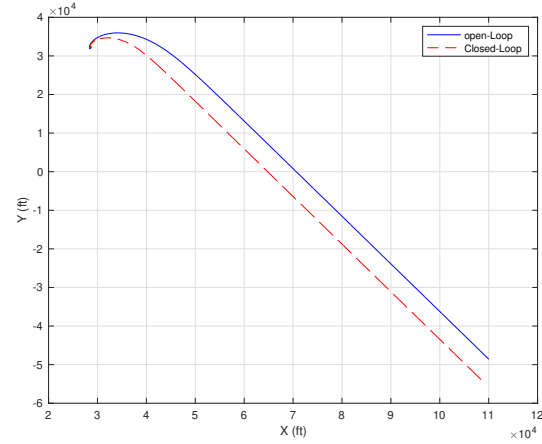


Fig. 4. The flying trajectory of the UAV towards the Drone Carrie ($\delta = 0.08$).

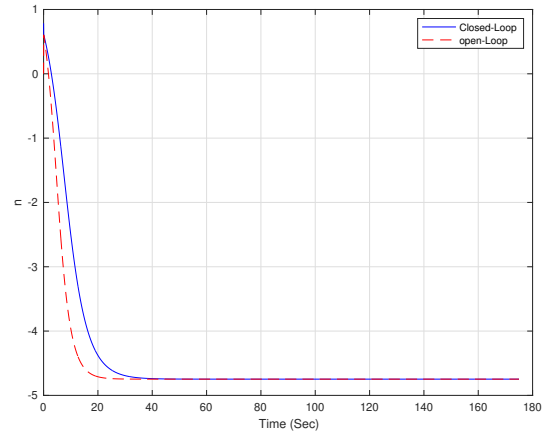


Fig. 5. Control Time History at ($\delta = 0.08$).

optimal route to reduce the flight time and save energy, since the in-flight power consumption is directly related to the total length of the flight path. Singular Perturbation technique (SPT) and optimal control methods are implemented to enable the UAV to intercept the drone carrier. Numerical results show that the proposed algorithm is effective in identifying the optimal travel path that leads to minimum travel time by using the closed loop numerical direct approach. Further development would include problem formulation in 3D with simulations under a practical environment such as ROS (Robot Operating System), which allows the sensor data to be considered and map out the surrounding environment to construct robust path planning.

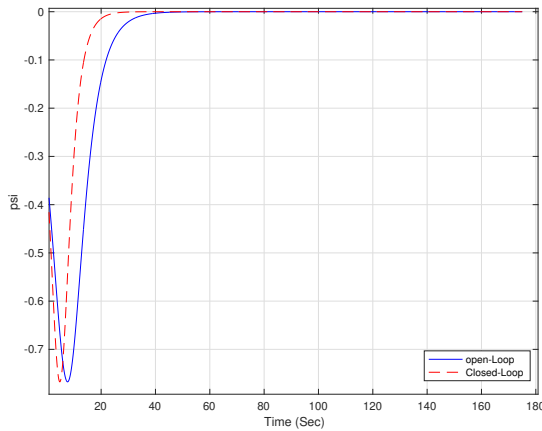


Fig. 6. Heading Time History at ($\delta = 0.08$).

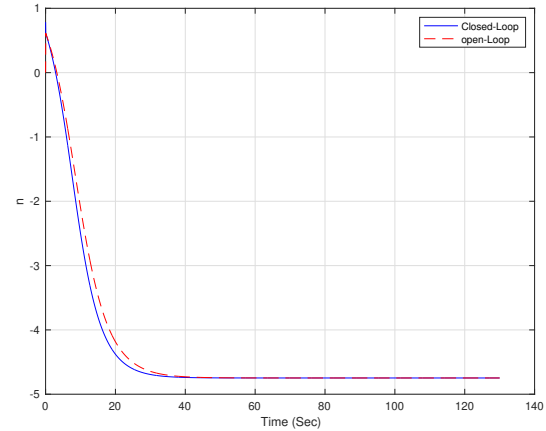


Fig. 8. Control Time History at ($\delta = 0.02$).

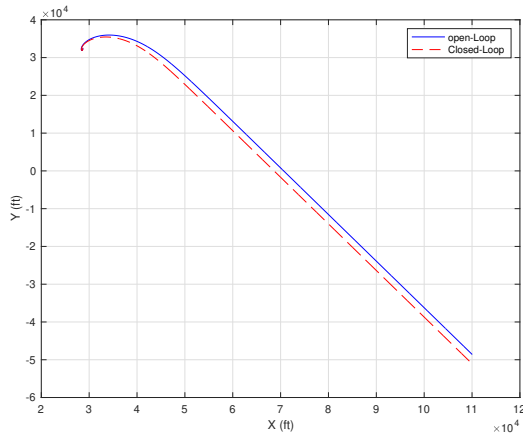


Fig. 7. The flying trajectory of the UAV towards the Drone Carrie ($\delta = 0.02$).

REFERENCES

- [1] P. Simek, J. Pavlik, J. Jarolimek, V. Ocenasek and M. Stoces, "Use of Unmanned Aerial Vehicles for Wildlife Monitoring", in *Proc. HAICTA*, Chania, Greece, 2017, pp. 795–804.
- [2] N. Kitpo and M. Inoue, "Early Rice Disease Detection and Position Mapping System using Drone and IoT Architecture", in *Proc. 12th-SEATUC*, Yogyakarta, Indonesia, 2018, pp. 978-983.
- [3] S.G. Gupta, M.M. Ghonge and P.M. Jawandhiya, "Review of unmanned aircraft system", *Technology*, vol. 2 (4), USA, 2013.
- [4] Amazon teases new details of planned prime air drone delivery service. [Online]. Available: <http://appleinsider.com/articles/15/11/30/>
- [5] Two delivery drones built google soon tested us. [Online]. Available: <http://www.techspot.com/news/62412>
- [6] M. Heutger, "Unmanned Aerial Vehicle in Logistics: A DHL Perspective on Implications and use Cases for the Logistics Industry", DHL Customer Solutions Innovation, Troisdorf, Germany, 2014.
- [7] K. Römer, "Tracking Real-world Phenomena with Smart Dust", *European Workshop on Wireless Sensor Networks*, Springer, Berlin Heidelberg, 2004, pp. 28–43.

- [8] D. Patil, M. Ansari, D. Tendulkar, R. Bhatlekar, V. N. Pawar and S. Aswale, "A Survey On Autonomous Military Service Robot," *ic-ETITE*, Vellore, India, 2020, pp. 1-7, doi: 10.1109/ic-ETITE47903.2020.78.
- [9] P. R. Palafox, M. Garzón, J. Valente, J. J. Roldán and A. Barrientos, "Robust Visual-Aided Autonomous Takeoff, Tracking, and Landing of a Small UAV on a Moving Landing Platform for Life-Long Operation", *Appl. Sci.* 2019, 9, 2661; doi:10.3390/app9132661.
- [10] L. Coutard and F. Chaumette, "Visual detection and 3D model-based tracking for landing on a aircraft carrier", in *Proc. IEEE International Conference on Robotics and Automation*, Shanghai, China, 2011, pp. 1746-1751.
- [11] L. Tan, J. Wu, X. Yang and S. Song, "Research on Optimal Landing path Planning Method between an UAV and a Moving Vessel", *mdpi, Appl. Sci.* 2019, 9, 3708.
- [12] F. Alarcon, M. Garcia, I. Maza, A. Viguria and A. Ollero, "A precise and gnss-free landing system on moving platforms for rotary-wing UAVs", *Sensors*, 2019, 19(4):886.
- [13] G. Pietro and A. Marini, "Air-to-air automatic landing for multirotor UAVs", *ING-IND/05 IMPIANTI E SISTEMI AEROSPAZIALI*, Politecnico Milano, Italy, 2018.
- [14] M. Jun and R. D'Andrea, "Path planning for Unmanned aerial vehicles in uncertainty and adversarial environments", In the Book Chapter of "Cooperative Control: Models, Applications and Algorithms", 2003.
- [15] K. Mina, "Fast nonlinear model predictive control for multi-copter attitude tracking on so (3)", 2015 IEEE Conference on Control Applications (CCA), IEEE, 2015.
- [16] M. Neunert, "Fast nonlinear model predictive control for unified trajectory optimization and tracking", 2016 IEEE international conference on robotics and automation (ICRA).
- [17] H. Tourajizadeh and O. Gholami, "Optimal Control and Path Planning of a 3PRS Robot Using Indirect Variation Algorithm", *Robotica*, 38(5), 903-924. doi:10.1017/S0263574719001152, 2020.
- [18] M. Alijani and A. Osman, "Autonomous Landing of UAV on Moving Platform: A Mathematical Approach," 2020 International Conference on Control, Automation and Diagnosis (ICCAD), 2020, pp. 1-6, doi: 10.1109/ICCADCAD49821.2020.9260498.
- [19] A. E. Bryson, "Applied Optimal Control: Optimization, Estimation and Control", Taylor Francis, 1975.
- [20] R. Yanushevsky, "Modern Missile Guidance", CRC Press, 2007. ISBN 978-1420062267.
- [21] D. S. Naidu and A. J. Calise, "Singular Perturbations and Time Scales in Guidance and Control of Aerospace Systems: A Survey", *Journal of Guidance Control and Dynamics* 24(6):1057-1078, DOI: 10.2514/2.4830, 2001.
- [22] <https://www.dji.com/it/mavic/info>